Molecular Carcinogenesis

The resveratrol analogue trimethoxystilbene inhibits cancer cell growth by inducing multipolar cell mitosis

Journal:	*Molecular Carcinogenesis*
Manuscript ID	MC-16-0242.R1
Wiley - Manuscript type:	Research Article
Date Submitted by the Author:	n/a
Complete List of Authors:	Traversi, Gianandrea; Universita degli Studi Roma Tre, Dipartimento di Scienze Fiore, Mario; Istituto di Biologia e Patologia Molecolari CNR, Via degli Apuli, 4, 00185 Roma, Italy Percario, Zulema; Universita degli Studi Roma Tre, Dipartimento di Scienze Degrassi, Francesca; Istituto di Biologia e Patologia Molecolari CNR, Via degli Apuli, 4, 00185 Roma, Italy Cozzi, Renata; Universita degli Studi Roma Tre, Dipartimento di Scienze
Keywords:	resveratrol analogues, tubulin polymerization, cancer cell growth, apoptosis, mitotic catastrophe

The resveratrol analogue trimethoxystilbene inhibits cancer cell growth by inducing multipolar cell mitosis.

Gianandrea Traversi[1], Mario Fiore[2], Zulema Percario[1], Francesca Degrassi[2]* and Renata Cozzi[1]*

[1]Dipartimento di Scienze, Università "Roma TRE", Viale G. Marconi 446, 00146 Roma, Italy

[2]Istituto di Biologia e Patologia Molecolari CNR, Via degli Apuli, 4, 00185 Roma, Italy

Keywords: resveratrol analogues tubulin polymerization cancer cell growth apoptosis mitotic catastrophe

*Correspondence:

Renata Cozzi, Viale G. Marconi 446, 00146 Roma Italy email: renata.cozzi@uniroma3.it

Francesca Degrassi, Via degli Apuli 4, 00185 Roma, Italy email: francesca.degrassi@uniroma1.it

Abstract

Natural compounds are extensively studied for their potential use in traditional and non-traditional medicine. Several natural and synthetic Resveratrol analogues have shown interesting biological activities in the field of cancer chemoprevention. In the present study, we have focused on the ability of Resveratrol and two methoxylated derivatives (Trimethoxystilbene and Pterostilbene) to inhibit human cancer cell growth particularly analyzing their ability to interfere with tubulin dynamics at mitosis. We show that Trimethoxystilbene, differently from Resveratrol and Pterostilbene, alters microtubule polymerization dynamics in HeLa cells specifically inducing multipolar spindles and mitotic arrest coupled to a reduction of cell growth and an increase in apoptotic death by mitotic catastrophe. This work demonstrates that the structural modification of Rsv causes substantial changes in the mechanism of action of the derivatives. The presence of three extra methyl groups renders Trimethoxy very efficient in impairing cell proliferation by inducing mitotic catastrophe in cancer cells.

Introduction

Natural compounds are extensively studied for their potential use in traditional and non-traditional medicine, including the management of oncological diseases. Among them Resveratrol (Rsv, 3,4',5-trihydroxystilbene), a natural stilbene, has been thoroughly analyzed for its anticarcinogenic and chemopreventive activity in a number of tumour cell lines and in phase 1 clinical trials [1,2]. In spite of the great amount of data currently available, many questions have been raised about the efficacy of this molecule [3]. Furthermore, Rsv low oral bioavailability and rapid metabolism represent a limitation for its in vivo use [4,5].

Accordingly, several natural and synthetic Rsv analogues have been tested against many cancer cell lines, often showing a greater antiproliferative activity [6]. For example, methoxy-derivatives, where Rsv hydroxyl groups are substituted with methoxyl ones, show a higher metabolic stability than Rsv [7]. Moreover, Pterostilbene (Ptero, trans-3,5-dimethoxy-4'-hydroxystilbene) and Trimethoxystilbene (Trimethoxy, trans-3,5,4'-trimethoxystilbene), which present two and three methoxyl groups respectively, show increased lipophilicity, resulting in better bioavailability, and possess higher antioxidant properties than the parental compound resveratrol [6,8]. Furthermore, Trimethoxy seems to exhibit an higher anticancer potency than Rsv, inhibiting cancer cell proliferation and metastasis and increasing apoptotic cell death [9].

One important target for the antiproliferative activity exerted by different compounds is microtubule dynamics due to the important role played by microtubule assembly and disassembly in mitotic processes [10]. Antimitotic molecules bind tubulin at various binding sites acting as microtubule stabilizers or destabilizers. Microtubule destabilizers inhibit tubulin polymerization, thereby leading cells to mitotic arrest and eventually to apoptotic death [11]. As far as Rsv analogues, literature data show that Trimethoxy acts as an anti-mitotic drug by blocking microtubule dynamics [12-15], in particular integrating within the colchicine-binding hydrophobic pocket in tubulin as showed by docking studies [16]. Recently, our group showed that Trimethoxy, but not Ptero, induces a strong delay in mitotic progression increasing the fraction of pro-metaphases and metaphases with a concomitant decrease in both prophases and ana/telophases in proliferating non-tumoral mammalian cells [17].

In the present study we have focused on the ability of Rsv and its two methoxylated derivatives, Ptero and Trimethoxy, to inhibit human cancer cell growth. To this purpose, we have analyzed the modulation of cell proliferation and mitosis progression in HeLa cells. Furthermore, the interference of the three molecules with microtubule dynamics at mitosis has been analyzed together with the induction of cell death. Here, we provide evidence that the structural modification of Rsv causes substantial changes in the mechanism of action of the derivatives. The presence of three extra methyl groups renders Trimethoxy very efficient in impairing cell growth by disrupting mitotic spindle structure and inducing mitotic catastrophe in cancer cells.

Materials and methods

Chemicals and reagents. Cell cultures and treatments

Resveratrol (Sigma–Aldrich), Pterostilbene (trans-3,5-dimethoxy-4'-hydroxystilbene) (Sigma–Aldrich) and Trimethoxystilbene (trans-3,5,4'-trimethoxystilbene) (Enzo Life Sciences) were dissolved in DMSO immediately before use and supplied to cell cultures at two concentrations, 20 and 80 µM. DMSO never exceeded 0.02% in the cultures. HeLa cells were maintained in Dulbecco's Modified Eagle Medium (DMEM) High Glucose supplemented with 10% fetal bovine serum, 2% penicillin/streptomycin solution, 1% l-glutamine, 0.1% gentamicin in a 37°C humidified incubator with 5% CO2. CHO cells were maintained in Ham's F-10 medium supplemented with 10% fetal bovine serum, 2% penicillin/streptomycin solution, 1% l-glutamine, 0.1% gentamicin in a 37°C humidified incubator with 5% CO2. All reagents were purchased from Euroclone (Milan, Italy).

Assembly of microtubules after cold treatment in CHO cells

2×10^5 CHO cells were seeded on glass coverslips in 35-mm Petri dishes the day before the experiment. The cells were incubated for 2 hrs on ice; then the cold medium was replaced with warm DMEM containing or not Rsv or Trimethoxy (80µM) and the samples were incubated at 37°C for 10 or 30 minutes. Then, the slides were rinsed in PHEM buffer [60 mM piperazine-N,N-bis(2-ethanesulfonic acid), 25 mM HEPES, pH 6.9, 10 mM EGTA, and 4 mM MgSO4] and fixed in 0.5% Triton-X in PHEM buffer with 3.7% formaldehyde; samples were rinsed in PBS and post-fixed in ice-cold MetOH for 5 min. After fixation, samples were rinsed again, blocked for 30 min in 5% goat serum and incubated at room temperature for 2 hrs with primary antibodies diluted in 5% goat serum. Primary antibodies were anti-α-tubulin (Sigma-Aldrich) and anti-γ-tubulin (Sigma-Aldrich) diluted 1:500 and 1:1000, respectively; 4 washings of 5 min at room temperature in PBS with 0.1 % Tween20 were carried out. Cells were then incubated at room temperature for 45 min with secondary antibodies diluted in 5% goat serum. Secondary antibodies were Alexa 488 anti-rabbit

(Molecular Probes) and X-Red anti-mouse (Jackson Laboratories) antibody diluted 1:1500 and 1:800, respectively. 4 washings of 5 minutes at room temperature in PBS with 0.1 % Tween20 were carried out, and samples were rinsed in PBS. DNA was counterstained in 0.05 µg/ml 4,6-diamidino-2-phenylindole (DAPI, Sigma, St Louis, MO, USA). Cells were viewed under an Olympus AX70 microscope using a 100×/1.35NA objective. Images were acquired using a CCD camera (Tucsen Photonics, China) controlled by ISCapture software.

Confocal microscopy of mitotic microtubules and centrosomes in CHO and HeLa cells

2×10^5 CHO or HeLa cells were seeded on glass coverslips in 35-mm Petri dishes and the following day cells were treated for 2 hours with different concentrations of the different molecules. At the end of the treatment cells were processed as described in section 2.2. Primary antibodies were anti-α-tubulin (Sigma-Aldrich) and anti-kinetochore serum (CREST, Antibodies Inc., Davis, CA, USA) diluted 1:500 and 1:100, respectively or anti-α-tubulin and γ- tubulin (Sigma-Aldrich). 4 washings of 5 minutes in PBS2- with 0.1 % Tween20 were carried out at room temperature. Secondary antibodies were X-Red anti-mouse (Jackson Laboratories) and Alexa 488 anti-human (Molecular Probes) antibody diluted 1:800 and 1:1500, respectively. DNA was counterstained with 0.05 µg/ml DAPI (Sigma, St Louis, MO, USA) for CHO cells or with fluorescent RedDot™2 dye (Biotium, Inc) diluted 1:200 for HeLa cells. Cells were viewed under a Leica TCS SP5 confocal microscope and processed with LAS AF version 1.6.3 software (Leica Microsystems). To prevent cross emission, specific lasers (488 nm, 546 nm and 633 nm) were activated in sequential mode during acquisition. Images shown are 3D projections of z-stacks from ≈ 20 confocal sections acquired at 0.5 µm intervals.

Flow cytometry for cell cycle and apoptosis analysis in Hela cells

5×10^5 HeLa cells were seeded in 25 cm2 flasks the day before the experiments. Cells were treated for 24 and 48 hours with Rsv , Ptero or Trimethoxy (20 and 80 µM). At the end of treatment cells were trypsinized, washed with PBS and fixed in a 1:1 cold methanol: PBS mixture. After extensive washing, cells were resuspended in PBS containing 20 µg/ml propidium iodide and analyzed for their DNA content (red fluorescence at 620 nm). Flow cytometric analysis was performed using an Epics XL apparatus (Beckman Coulter) equipped with a 15 mW argon laser with a 488 nm wavelength excitation light. Ten thousand events were collected from each sample. DNA content was analyzed using WinMDI 2.9 software.

Cell growth and Mitotic index in Hela cells

2×10^5 HeLa cells were seeded in 25 cm2 flask the day before the experiment; cells were then treated for 24, 40, 48 and 72 hours with Rsv, Ptero or Trimethoxy (80 µM). At the end of the treatment, an aliquot of each sample was collected in order to count the number of cells through a Z1 Counter (Beckman Coulter). The remaining cell suspension was centrifuged, incubated in a 3:1 mixture distilled water/complete DMEM for 5 minutes and fixed in a 3:1 methanol/glacial acetic acid mixture for 5 minutes. Finally, cells were seeded on slides and then stained with conventional

Giemsa method. For each experimental point 1000 cells were analyzed identifying cells in mitosis and interphase.

Multinucleated cells analysis in HeLa cells

$1x10^5$ HeLa cells were seeded on glass coverslips in 35-mm Petri dish the day before the experiment; cells were treated for 24, 48, 72 and 96 hours with Trimethoxy (20 and 80 µM). At the end of the treatment cells were fixed with methanol for 30 minutes at 4 °C and then stained with Giemsa. For each experimental point 1000 cells were analyzed.

Statistical analysis

Data are presented as the mean of at least three independent experiments along with standard error (SE). The unpaired t-test was applied to compare the data. Probability values (p) <0.05 were considered statistically significant. Statistical analysis of data was done by GraphPad software Instat version 3.02 (GraphPad Software, San Diego, CA).

Results

Trimethoxy , but not Rsv and Ptero, affects tubulin polymerization in CHO and HeLa cells

In a previous paper we showed that Trimethoxy induces a strong delay in mitotic progression in CHO cells, blocking cells in prometaphase [17]. Since these data suggested an activation of the spindle assembly checkpoint (SAC) possibly due to an interference of Trimethoxy with microtubule dynamics, we examined the microtubule-based mitotic spindle structure by confocal microscopy after treatment of CHO cells with 20 µM Rsv, Ptero, Trimethoxy or nocodazole (as positive control) for 2 hours. Rsv- and Ptero-treated CHO cells showed a typical mitotic microtubule organization with fusiform spindles and aligned kinetochore signals similar to untreated cells (Fig.1A). On the contrary, mitotic spindles in Trimethoxy-treated cells showed completely disorganized microtubule arrays with fewer microtubules of various lengths. Microtubules pointed towards different directions, they did not interact with kinetochores in the central region but overpassed kinetochores. Finally, spindle microtubules in nocodazole-treated CHO cells were completely depolymerized as expected for a strong spindle poison (Fig.1A). On the whole, these results indicated that only the three methoxy- derivative Trimethoxy has the ability to alter microtubule polymerization dynamics, although to a lesser extent than the model compound nocodazole.

In order to assess microtubule polymerization in the presence of Trimethoxy, we tested whether Rsv or Trimethoxy affected microtubule assembly by observing the reassembly pattern of cold-depolymerized spindle microtubules in CHO cells. At low temperature (4°C) microtubules depolymerize into dimeric tubulin and at higher temperature (37°C) tubulin polymerizes into microtubules. We used this property to identify the effect of the different treatments on this reassembly pattern in mitotic cells. After cold treatment (T0) the majority of mitotic cells showed depolymerized microtubules (Fig.1B). CHO cells were then incubated with fresh warm medium containing or not Rsv or Trimethoxy for 10 and 30 minutes (T10 and T30). In the absence of drugs, cold-depolymerized microtubules progressively reassembled from centrosomes to form a bipolar microtubule spindle (Fig.1B), so that after 30 minutes about 80% of cells showed full microtubule growth. In the presence of Trimethoxy (80 µM) microtubules failed to reassemble; after 30 minutes (T30) in warm medium supplemented with Trimethoxy almost 100% of mitotic cells showed no microtubule growth. On the contrary, CHO cells treated with Rsv showed a progressive time-dependent polymerization of tubulin so that after 30 minutes in warm medium supplemented with Rsv 63% of cells showed polymerized spindle microtubules (80% in untreated cells). These data suggest that Trimethoxy prevents microtubule assembly inside the cell.

Since the interest in an antimitotic activity of Trimethoxy is principally due to the assumption that this molecule could be effective against cancer cells, we analyzed the effect of Rsv and its methoxy-derivatives on cellular microtubules in human cervical cancer cells (HeLa) by confocal microscopy (Fig.2A). Spindle microtubules were less compact and the mitotic spindle was heavily disorganized in Trimethoxy-treated Hela cells with a large fraction of chromosomes remaining at the spindle poles. On the contrary, spindle microtubules were regular and chromosome aligned at the metaphase plate in control, Rsv- or Ptero-treated HeLa cells. In fact, we observed less than 10% of cells with altered microtubule polymerization in control, Rsv- or Ptero-treated cells whereas more than 80% of cells exhibited disorganized or depolymerized mitotic spindles in Trimethoxy-treated samples (Fig 2B).

Since centrosome hyper-amplification is common in cancer cells and substances affecting tubulin polymerization may cause centrosome number variation we determined whether HeLa cells showed an abnormal number of centrosomes after a 2 hour treatment with Rsv and its derivatives using γ tubulin as a centrosome marker (Fig 3A). We found that Trimethoxy-treated HeLa cells have a significantly

higher proportion of cells with mitosis showing >2 centrosomes (64% compared to 20% in untreated cells $p<0.01$) with a wide variety of centrosome numbers (Fig.3B). The number of centrosomes remained unchanged after Rsv or Ptero treatments. These observations lead to the conclusion that microtubule disorganization in Trimethoxy-treated HeLa cells produces alterations in centrosome number as an excess of mitotic centrosomes.

Trimethoxy, but not Rsv and Ptero, is highly effective in inducing apoptotic cell death from mitosis in HeLa cells.

In order to evaluate the consequences of the mitotic spindle damaging activity exerted by Trimethoxy (but not by Rsv or Ptero) on cancer cell proliferation, we treated HeLa cells with the three molecules for different times and analyzed cell growth, mitotic index and cell cycle progression.

Figure 4A shows the effect of 24, 40, 48 and 72 hours treatment with 80 µM of Rsv, Ptero, Trimethoxy on cell growth. All substances induced a drastic reduction in cell growth particularly evident at 48 and 72 hours. When mitotic index was examined we observed a dramatic increase in the frequency of mitotic cells until 40 hour treatment with Trimethoxy ($p<0.05$ and $p<0.001$ respectively at 24 and 40 hours); thereafter the mitotic fraction rapidly decreased without reaching control values even after 72 hour treatment. On the contrary, both Rsv and Ptero treatment decreased the frequency of mitoses compared to controls at all treatment times (Fig. 4A). These data highlight a profound difference in the mechanism of action of Trimethoxy as compared to Rsv or Ptero and demonstrate that similar growth inhibitory effects may be linked to different molecular mechanisms for structurally similar compounds.

To better understand the different modes of action of the three molecules we examined the modulation of cell cycle progression at two different treatment times through flow cytometry (Fig. 4B). Both 20 and 80 µM Trimethoxy induced a progressive accumulation of HeLa cells in the G2/M phase with a concomitant reduction of cells in the G1 and S phases. This effect was particularly evident after a 48 hour treatment with 80 µM Trimethoxy where we found 95% of cells in G2/M vs 25% in untreated cells (Fig. 4C). As far as Rsv and Ptero treatment, both substances induced a delay in cell cycle progression through S phase, particularly after a 48 hour

treatment: 68% and 58% of cells were in S phase, respectively, vs 13.5% in untreated cells (Fig.4C).

To know the fate of the cells arrested in mitosis by Trimethoxy treatment we examined the level of apoptosis induced after 24 and 48 hour treatment through flow cytometry and compared the apoptosis-inducing ability of Trimethoxy to that of Rsv and Ptero (Fig 5A). While 20 µM Trimethoxy did not increase the frequency of hypodiploid cells over the control values, 80 µM Trimethoxy potently produced hypodiploidy at 48 and 72 hours (Fig. 5B). On the contrary, 80 µM Rsv or Ptero did not significantly increase the fraction of hypodiploid cells at 48 h and were less efficient in producing hypodiploid cells at 72 hours. Altogether, these data demonstrate that Trimethoxy efficiently arrests cells in mitosis up to 40 h (Fig 4A) and induces massive DNA fragmentation at later times (Fig 5B), suggesting that mitotically arrested cells undergo apoptosis upon Trimethoxy exposure. This temporal sequence suggests mitotic catastrophe as the type of cell death elicited by Trimethoxy. Mitotic catastrophe has been defined as a type of cell death that results from an abnormal mitosis and is associated with the induction of the apoptotic process directly from mitosis or the formation of large cells with multiple nuclei/micronuclei i.e. multinucleated cells [18]. To confirm mitotic catastrophe as the mechanism behind Trimethoxy-induced apoptosis we analyzed the induction of binucleated and multinucleated cells (examples in Fig. 6A) at different treatment times. The temporal and quantitative dynamics of multinucleation induction paralleled the flow cytometric detection of apoptosis for 80 µM Trimethoxy, demonstrating that mitotic catastrophe was induced. In agreement with flow cytometry data, no induction of multinucleation was, instead, observed in 20 µM Trimethoxy treated cells (Fig. 6B).

On the whole the above results indicate that the reduction in cell growth caused by the three molecules is due to different modes of action: Rsv and Ptero cause a delay of cell cycle progression during the S phase while Trimethoxy induces an accumulation of HeLa cells in mitosis that well agrees with its ability to interfere with tubulin polymerization and mitotic spindle organization. Most of the cells arrested in mitosis undergoes mitotic catastrophe, demonstrating that Trimethoxy is a very potent inducer of apoptotic cell death from mitosis.

Discussion

It has been reported through immunofluorescence analysis of cancer cells that Trimethoxy, but not Rsv, causes depolymerization of the microtubule network of interphase cells [12]. This activity was linked to a direct interaction with the colchicine-binding hydrophobic pocket in tubulin [12]. Molecular docking studies performed by Mazuè and coworkers [16] showed that most of the synthetic methylated derivatives of Rsv and (Z)-polymethoxy isomers interact with the colchicine-tubulin binding site. This is the tubulin site where many of the natural and synthetic anticancer agents are believed to act [19]. A series of Rsv derivatives possessing chalcone moiety were evaluated as potential antitubulin agents. In particular, the alkylated derivatives showed the most potent inhibitory effect against tubulin polymerization coupled to antiproliferative activity in cancer cells [20].

In this study we demonstrate that Trimethoxy interferes with tubulin polymerization both in normal and in cancer cells, inhibiting microtubule polymerization on mitotic cells. This activity leads to mitotic spindle disruption and causes an arrest of cancer cells in mitosis. Consequently, cancer cell proliferation is abolished, due to the activation of mitotic catastrophe, a mitotic-related cell death pathway.

Here, we also show for the first time that not only Rsv but also Ptero, a dimethoxy derivative of Rsv, do not interfere with tubulin. This is in agreement with literature data reporting the crucial role of 3,4,5-trimethoxyphenil unit as a potent fragment to interact with tubulin [10]. Several compounds possessing this fragment bind tubulin within the colchicine binding site at m M concentrations [21].

We further demonstrate the capacity of Trimethoxy to increase the number of centrosomes after short time treatments of HeLa cells. The centrosome contributes to the organization and orchestration of mitosis and centrosome accumulation is very frequently present in cancer cells where causes aberrant mitoses and chromosome mis-segregation [22]. It is well known that cancer cells cluster supernumerary centrosomes to form functional bipolar spindle since centrosome amplification or fragmentation lead to multipolar spindles, which may cause aneuploidy and reduced cell viability [23]. Our findings clearly demonstrate that Trimethoxy produces spindle multipolarity, although we cannot infer whether Trimethoxy causes an inhibition of centrosome clustering or induces centrosome fragmentation. However, since our data show that Trimethoxy inhibits microtubule

dynamics we can speculate that the compound inhibits centrosome clustering. In fact, attenuation of microtubule dynamics is the mode of action of well-known centrosome declustering drugs, such as bromonoscapine and griseofulvin, which represent cancer cell-selective and efficacious chemotherapeutic agents [23].

Induction of multipolarity by centrosome declustering [24,25] or loss of spindle pole integrity [26,27] has been proposed as a powerful pro-apoptotic death mechanism, since chromosome segregation in multipolar spindles is heavily aberrant so that daughter cells are unviable and undergo mitotic catastrophe. In our work Trimethoxy has proven very effective in producing spindle multipolarity, DNA hypodiploidy and multinucleation, demonstrating that its potential anti-cancer activity is mediated by its ability to produce multipolar spindles that drive cancer cells into mitotic catastrophe.

Interestingly, when we analyzed the effect of Rsv and derivatives on cell proliferation we found that all the molecules cause a delay in cell cycle progression but with different modalities. In fact, Rsv causes an accumulation of cells in S phase confirming our and other groups' results obtained in different cancer cells [28-30]. Similar to Rsv, Ptero treatment delays cell transition in S phase, while Trimethoxy strongly increases the percentage of cells in mitotic cells in a dose- and time-dependent manner. This last result, in agreement with those obtained in normal cells [17], is due to tubulin depolymerization which causes in turn the block of mitotic progression. In fact Trimethoxy, but not Rsv and Ptero, induces a significant increase in mitotic index, which reaches a peak and then strongly declines at prolonged treatment times. Furthermore, the increase in mitotic index and the block in M phase are coupled to a reduction of cell growth and an increase in apoptotic death. Also Rsv and Ptero induce apoptotic cell death at later time, although less effectively. In particular, Rsv-induced apoptotic death could be mediated by its topoisomerase poisoning activity mainly exerted during the S phase [31].

In conclusion, we show here that Resveratrol and its methoxy-derivatives are all able to affect cell cycle progression in cancer cells. However, Trimethoxy, differently from Rsv and Ptero, acts as a tubulin depolymerizing agent, which specifically induces mitotic arrest shifting the balance from cell survival to cell death. In our knowledge this is the first report which clearly highlights the link between induction

of mitotic arrest, through tubulin dynamic interference, and cell death, through mitotic catastrophe, induced by Trimethoxy treatment in HeLa cells.

The induction of mitotic catastrophe by Trimethoxy could be usefully exploited for the development of therapeutic strategies to treat aggressive types of cancers such as, for example, glioblastomas that have fast proliferation rates and often develop resistance to established anticancer therapies.

On the whole, our results provide important new insights into the mechanism of action of Rsv methoxy-derivatives suggesting that the modification of hydroxyl groups in the Rsv-stilbene motif, while increasing bioavailability, can effectively produce more active molecules with new clinical potential for fighting cancer.

References

1. Shukla Y, Singh R. Resveratrol and cellular mechanisms of cancer prevention. Ann N Y Acad Sci 2011;1215:1-8.
2. Gescher A, Steward WP, Brown K. Resveratrol in the management of human cancer: how strong is the clinical evidence? Ann N Y Acad Sci 2013;1290:12-20.
3. Signorelli P, Ghidoni R. Resveratrol as an anticancer nutrient: molecular basis, open questions and promises. J Nutr Biochem 2005;16(8):449-466.
4. Cottart CH, Nivet-Antoine V, Beaudeux JL. Review of recent data on the metabolism, biological effects, and toxicity of resveratrol in humans. Mol Nutr Food Res 2014;58(1):7-21.
5. Carter LG, D'Orazio JA, Pearson KJ. Resveratrol and cancer: focus on in vivo evidence. Endocr Relat Cancer 2014;21(3):R209-225.
6. Fulda S. Resveratrol and derivatives for the prevention and treatment of cancer. Drug Discov Today. Volume 15. England: 2010 Elsevier Ltd; 2010. p 757-765.
7. Zhang W, Go ML. Quinone reductase induction activity of methoxylated analogues of resveratrol. Eur J Med Chem 2007;42(6):841-850.
8. Rossi M, Caruso F, Antonioletti R et al. Scavenging of hydroxyl radical by resveratrol and related natural stilbenes after hydrogen peroxide attack on DNA. Chem Biol Interact 2013;206(2):175-185.
9. Aldawsari FS, Velazquez-Martinez CA. 3,4',5-trans-Trimethoxystilbene; a natural analogue of resveratrol with enhanced anticancer potency. Invest New Drugs 2015;33(3):775-786.
10. Negi AS, Gautam Y, Alam S et al. Natural antitubulin agents: importance of 3,4,5-trimethoxyphenyl fragment. Bioorg Med Chem 2015;23(3):373-389.
11. Jordan MA, Wilson L. Microtubules as a target for anticancer drugs. Nat Rev Cancer 2004;4(4):253-265.
12. Schneider Y, Chabert P, Stutzmann J et al. Resveratrol analog (Z)-3,5,4'-trimethoxystilbene is a potent anti-mitotic drug inhibiting tubulin polymerization. Int J Cancer 2003;107(2):189-196.
13. Hong YB, Kang HJ, Kim HJ et al. Inhibition of cell proliferation by a resveratrol analog in human pancreatic and breast cancer cells. Exp Mol Med 2009;41(3):151-160.
14. Scherzberg MC, Kiehl A, Zivkovic A et al. Structural modification of resveratrol leads to increased anti-tumor activity, but causes profound changes in the mode of action. Toxicol Appl Pharmacol 2015;287(1):67-76.

15. Nguyen CB, Kotturi H, Waris G et al. (Z)-3,5,4'-Trimethoxystilbene Limits Hepatitis C and Cancer Pathophysiology by Blocking Microtubule Dynamics and Cell Cycle Progression. Cancer Res 2016.
16. Mazue F, Colin D, Gobbo J et al. Structural determinants of resveratrol for cell proliferation inhibition potency: experimental and docking studies of new analogs. Eur J Med Chem 2010;45(7):2972-2980.
17. Traversi G, Fiore M, Leone S et al. Resveratrol and its methoxy-derivatives as modulators of DNA damage induced by ionising radiation. Mutagenesis 2016;31(4):433-441.
18. Vitale I, Galluzzi L, Castedo M, Kroemer G. Mitotic catastrophe: a mechanism for avoiding genomic instability. Nat Rev Mol Cell Biol 2011;12(6):385-392.
19. Bhattacharyya B, Panda D, Gupta S, Banerjee M. Anti-mitotic activity of colchicine and the structural basis for its interaction with tubulin. Med Res Rev 2008;28(1):155-183.
20. Ruan BF, Lu X, Tang JF et al. Synthesis, biological evaluation, and molecular docking studies of resveratrol derivatives possessing chalcone moiety as potential antitubulin agents. Bioorg Med Chem 2011;19(8):2688-2695.
21. Luduena RF, Roach MC. Tubulin sulfhydryl groups as probes and targets for antimitotic and antimicrotubule agents. Pharmacol Ther 1991;49(1-2):133-152.
22. Cosenza MR, Kramer A. Centrosome amplification, chromosomal instability and cancer: mechanistic, clinical and therapeutic issues. Chromosome Res 2016;24(1):105-126.
23. Ogden A, Rida PC, Aneja R. Let's huddle to prevent a muddle: centrosome declustering as an attractive anticancer strategy. Cell Death Differ 2012;19(8):1255-1267.
24. Kwon M, Godinho SA, Chandhok NS et al. Mechanisms to suppress multipolar divisions in cancer cells with extra centrosomes. Genes Dev 2008;22(16):2189-2203.
25. Galimberti F, Thompson SL, Liu X et al. Targeting the cyclin E-Cdk-2 complex represses lung cancer growth by triggering anaphase catastrophe. Clin Cancer Res 2010;16(1):109-120.
26. Orticello M, Fiore M, Totta P et al. N-terminus-modified Hec1 suppresses tumour growth by interfering with kinetochore-microtubule dynamics. Oncogene 2015;34(25):3325-3335.
27. Wang J, Li J, Santana-Santos L et al. A novel strategy for targeted killing of tumor cells: Induction of multipolar acentrosomal mitotic spindles with a quinazolinone derivative mdivi-1. Mol Oncol 2015;9(2):488-502.
28. Schneider Y, Vincent F, Duranton B et al. Anti-proliferative effect of resveratrol, a natural component of grapes and wine, on human colonic cancer cells. Cancer Lett 2000;158(1):85-91.
29. Larrosa M, Tomas-Barberan FA, Espin JC. Grape polyphenol resveratrol and the related molecule 4-hydroxystilbene induce growth inhibition, apoptosis, S-phase arrest, and upregulation of cyclins A, E, and B1 in human SK-Mel-28 melanoma cells. J Agric Food Chem 2003;51(16):4576-4584.
30. Leone S, Cornetta T, Basso E, Cozzi R. Resveratrol induces DNA double-strand breaks through human topoisomerase II interaction. Cancer Lett 2010;295(2):167-172.
31. Leone S, Basso E, Polticelli F, Cozzi R. Resveratrol acts as a topoisomerase II poison in human glioma cells. Int J Cancer 2012;131(3):E173-178.

Figure captions

Figure 1. *Effect of Rsv, Ptero and Trimethoxy on microtubule polymerization in CHO cells.* (A) Cells were treated with 20 µM Rsv, Ptero and Trimethoxy for 2 hours, fixed and stained with anti-α tubulin antibody (red) and anti-kinetochore serum (CREST, green). Nocodazole was used as positive control. 3D projections of confocal images of untreated and treated cells are shown. (B) CHO cells were incubated for 2 hours on ice, then immediately fixed (T0) or incubated at 37°C for 10 or 30 minutes (T10 and T30) in the presence or absence of Rsv or Trimethoxy (80 µM). Cells were stained with ant-α (red) and anti-γ tubulin (green) antibodies and DNA was stained with DAPI (blue). In the upper panel representative images of cells with completely depolymerized microtubules (MT), partially grown MT or fully polymerized MT are shown (white arrows); in the bottom panel the percentages of cells with different tubulin organization pattern in control and treated samples are reported. Values are the mean ± S.E. of three independent experiments. *p<0.05 ***p<0.001 as compared to the respective control using unpaired t-test

Figure 2. *Effect of Rsv, Ptero and Trimethoxy on microtubule polymerization in HeLa cells.* Cells were treated with Rsv, Ptero and Trimethoxy for 2 hours, fixed and stained with anti-α tubulin antibody (red) and DNA RedDot™2 dye (blue).

Nocodazole was used as positive control. (A) 3D projections of confocal images of untreated and treated mitotic cells are shown. (B) Percentages of cells with normal and depolymerized microtubules are shown.

Figure 3. *Alteration of centrosome number by Trimethoxy in HeLa cells.* Hela cells were treated with Rsv, Ptero or Trimethoxy (20 and 80 µM), fixed and stained with anti-α (red) and anti-γ tubulin (green). (A) 3D projections of confocal images of untreated and Trimethoxy treated mitotic cells are shown. (B) In the upper histograms the percentage of cells with 2 or more than 2 centrosomes is shown; in the lower histograms the number of cells with 3, 4, 5 and more than 6 centrosomes in control and Trimethoxy treated samples is shown. Values are the mean ± S.E. of three independent experiments. **p<0.01 as compared to the control using unpaired t-test

Figure 4. *Effect of Rsv, Ptero and Trimethoxy on cell growth and division in HeLa cells.* (A) Hela cells were treated for 24, 40, 48 and 72 hours with Rsv, Ptero and Trimethoxy (80 µM). At the end of the different treatment times, cells were counted for cell growth (upper panel) or fixed and stained with Giemsa for mitotic index measurement (lower panel). Values are the mean ± S.E. of three independent experiments. *p<0.05 ***p<0.001 as compared to the control using unpaired t-test (B) Flow cytometry analysis of cell cycle progression in HeLa cells treated with Rsv, Ptero or Trimethoxy (20 and 80 µM) for 24 and 48 hours. (C) In the histograms the distribution of the cells in the different cell cycle phases after 24 (upper panel) and 48 (lower panel) hour treatment is shown.

Figure 5. *Effect of Rsv, Ptero and Trimethoxy on apoptosis in HeLa cells.* Hela cells were treated for 24, 48 and 72 hours with 80 µM Rsv, Ptero or Trimethoxy (20 and 80 µM). At the end of treatments cells were harvested, fixed and subjected to flow cytometry to determine DNA content. (A) Representative profiles of DNA content distribution in control and treated samples are shown, using a logarithmic scale (X axis) in order to identify hypodiploid peaks. (B) In the histograms the percentages of hypodiploid cells in control and treated samples are shown. Values are the mean ± S.E. from three independent experiments. *p<0.05 **p<0.01 as compared to the control using unpaired t-test

Figure 6. *Induction of multinucleation by Trimethoxy in HeLa cells.* Hela cells were treated for 24,48, 72 and 96 hours with Trimethoxy (20 and 80 µM). At the end of treatments cells were fixed and stained with Giemsa. (A) Microscopic images showing cells with 1, 2, 3 or more nuclei. (B) In the histograms the percentage of binucleated or multinucleated cells is shown. Values are the mean ± S.E. from three independent experiments. *p<0.05 **p<0.01 *** p<0.001 as compared to the control using unpaired t-test

Supporting information

Figure S1. *Structure of the molecules.* (A) Resveratrol (B) Pterostilbene (C) Trimethoxystilbene

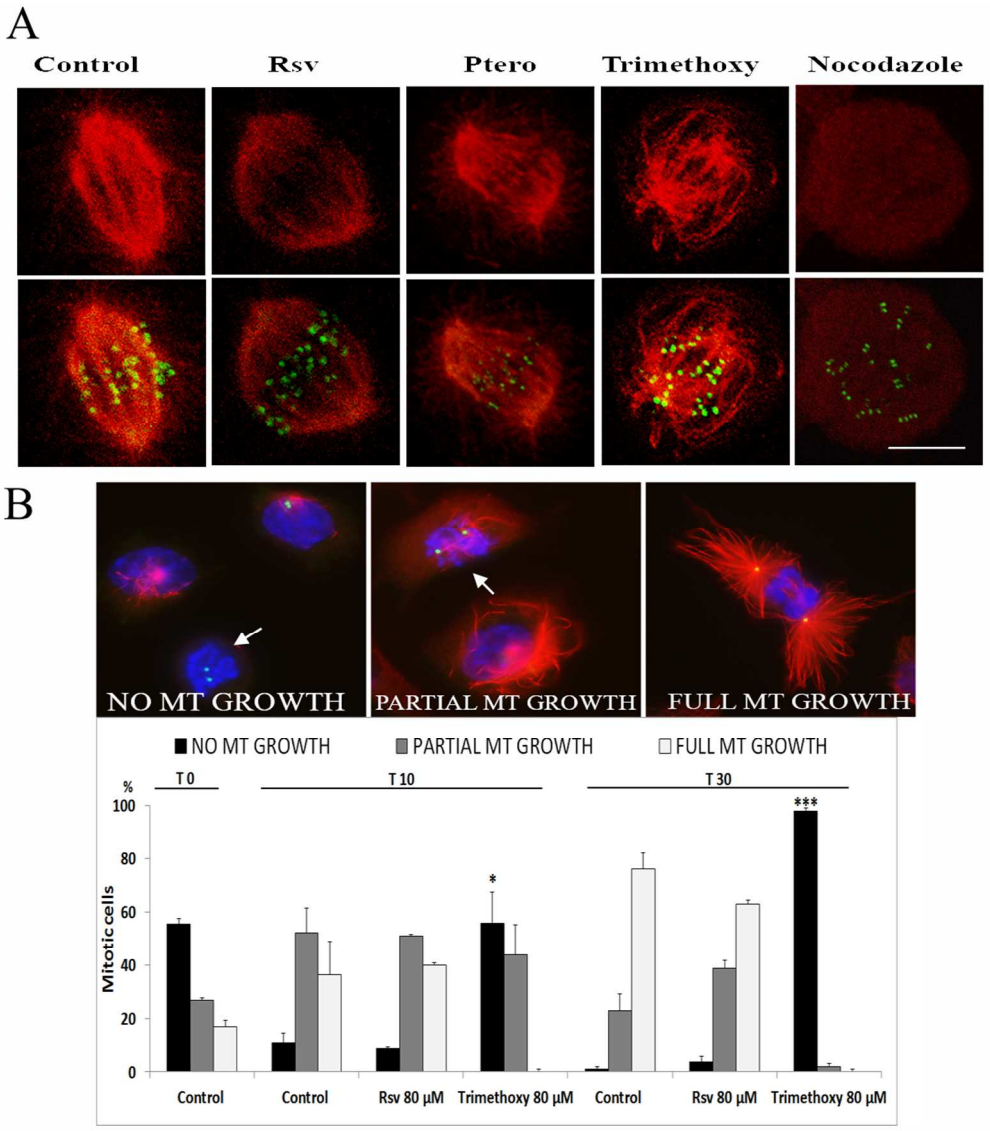

Figure 1. Effect of Rsv, Ptero and Trimethoxy on microtubule polymerization in CHO cells. (A) Cells were treated with 20 µM Rsv, Ptero and Trimethoxy for 2 hours, fixed and stained with anti-α tubulin antibody (red) and anti-kinetochore serum (CREST, green). Nocodazole was used as positive control. 3D projections of confocal images of untreated and treated cells are shown. (B) CHO cells were incubated for 2 hours on ice, then immediately fixed (T0) or incubated at 37°C for 10 or 30 minutes (T10 and T30) in the presence or absence of Rsv or Trimethoxy (80 µM). Cells were stained with ant-α (red) and anti-γ tubulin (green) antibodies and DNA was stained with DAPI (blue). In the upper panel representative images of cells with completely depolymerized microtubules (MT), partially grown MT or fully polymerized MT are shown (white arrows); in the bottom panel the percentages of cells with different tubulin organization pattern in control and treated samples are reported. Values are the mean ± S.E. of three independent experiments. *p<0.05 ***p<0.001 as compared to the respective control using unpaired t-test

106x122mm (300 x 300 DPI)

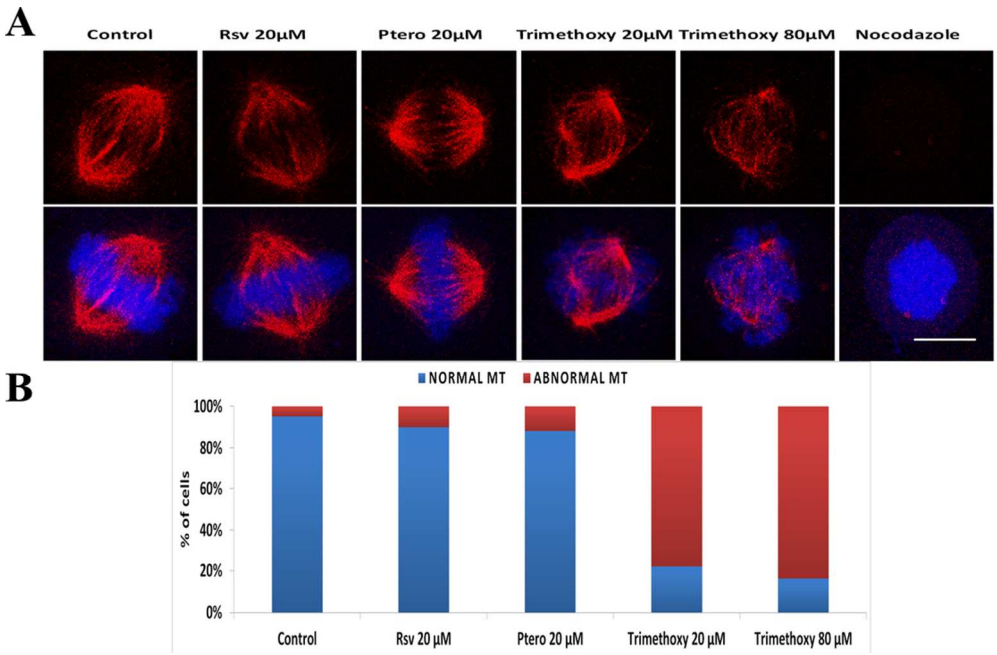

Figure 2. Effect of Rsv, Ptero and Trimethoxy on microtubule polymerization in HeLa cells. Cells were treated with Rsv, Ptero and Trimethoxy for 2 hours, fixed and stained with anti-α tubulin antibody (red) and DNA RedDot™2 dye (blue). Nocodazole was used as positive control. (A) 3D projections of confocal images of untreated and treated mitotic cells are shown. (B) Percentages of cells with normal and depolymerized microtubules are shown.

94x61mm (300 x 300 DPI)

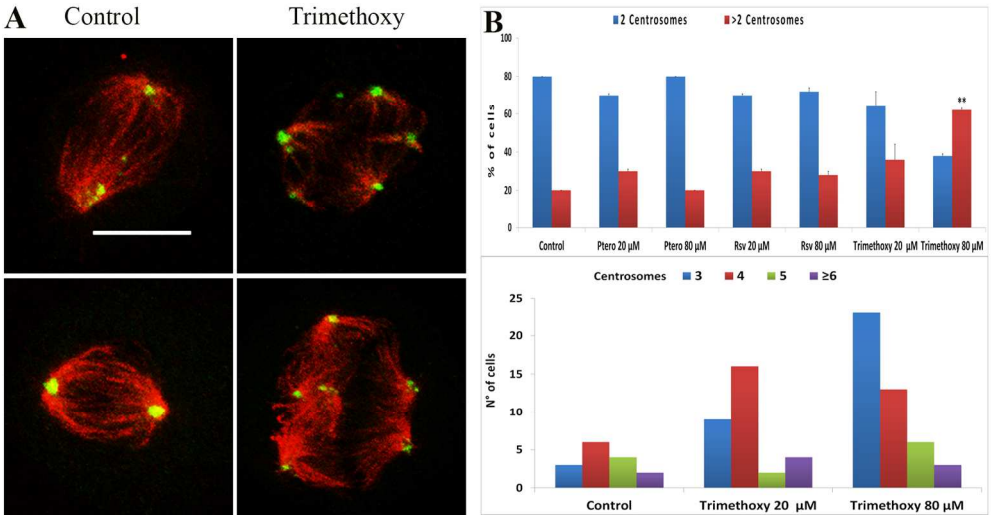

Figure 3. Alteration of centrosome number by Trimethoxy in HeLa cells. Hela cells were treated with Rsv, Ptero or Trimethoxy (20 and 80 µM), fixed and stained with anti-α (red) and anti-γ tubulin (green). (A) 3D projections of confocal images of untreated and Trimethoxy treated mitotic cells are shown. (B) In the upper histograms the percentage of cells with 2 or more than 2 centrosomes is shown; in the lower histograms the number of cells with 3, 4, 5 and more than 6 centrosomes in control and Trimethoxy treated samples is shown. Values are the mean ± S.E. of three independent experiments. **p<0.01 as compared to the control using unpaired t-test

156x80mm (300 x 300 DPI)

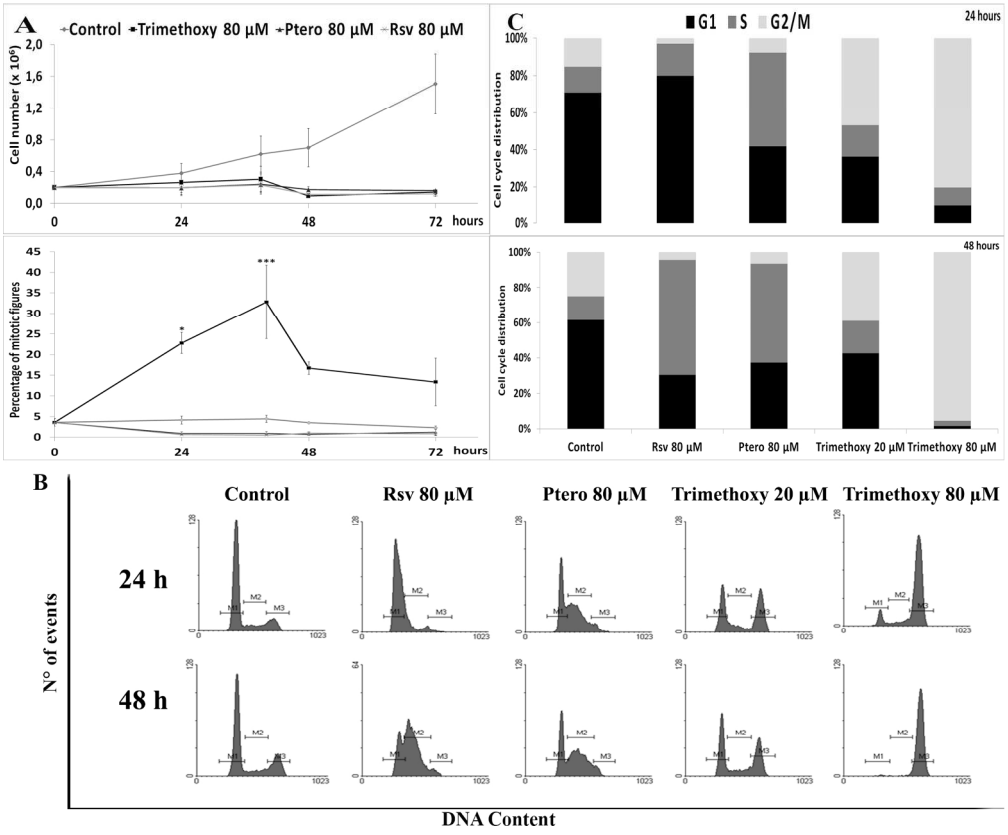

Figure 4. Effect of Rsv, Ptero and Trimethoxy on cell growth and division in HeLa cells. (A) Hela cells were treated for 24, 40, 48 and 72 hours with Rsv, Ptero and Trimethoxy (80 µM). At the end of the different treatment times, cells were counted for cell growth (upper panel) or fixed and stained with Giemsa for mitotic index measurement (lower panel). Values are the mean ± S.E. of three independent experiments. *p<0.05 ***p<0.001 as compared to the control using unpaired t-test (B) Flow cytometry analysis of cell cycle progression in HeLa cells treated with Rsv, Ptero or Trimethoxy (20 and 80 µM) for 24 and 48 hours. (C) In the histograms the distribution of the cells in the different cell cycle phases after 24 (upper panel) and 48 (lower panel) hour treatment is shown.

180x150mm (300 x 300 DPI)

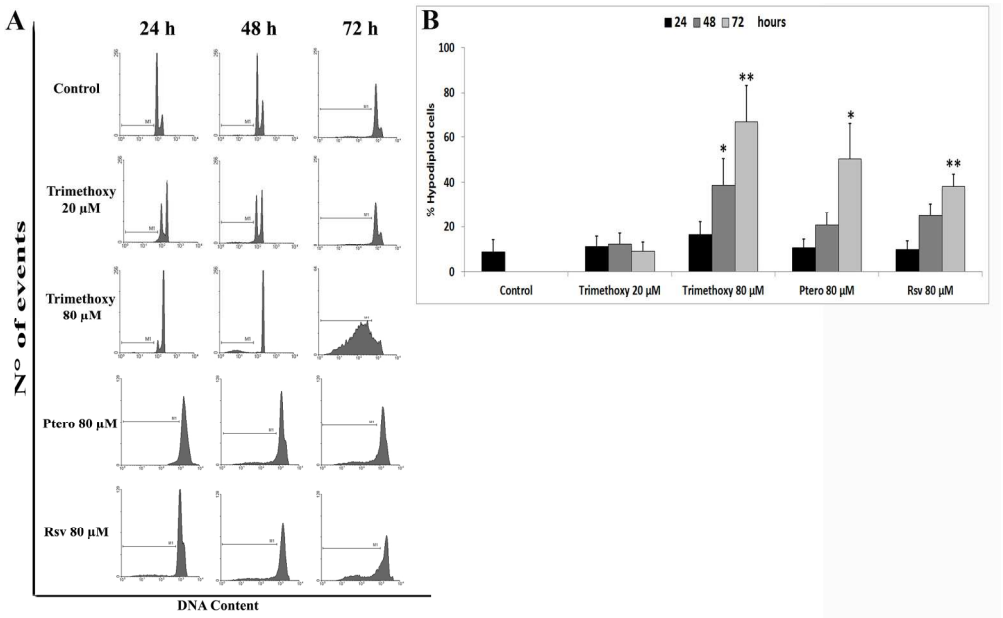

Figure 5. Effect of Rsv, Ptero and Trimethoxy on apoptosis in HeLa cells. Hela cells were treated for 24, 48 and 72 hours with 80 µM Rsv, Ptero or Trimethoxy (20 and 80 µM). At the end of treatments cells were harvested, fixed and subjected to flow cytometry to determine DNA content. (A) Representative profiles of DNA content distribution in control and treated samples are shown, using a logarithmic scale (X axis) in order to identify hypodiploid peaks. (B) In the histograms the percentages of hypodiploid cells in control and treated samples are shown. Values are the mean ± S.E. from three independent experiments. *p<0.05 **p<0.01 as compared to the control using unpaired t-test

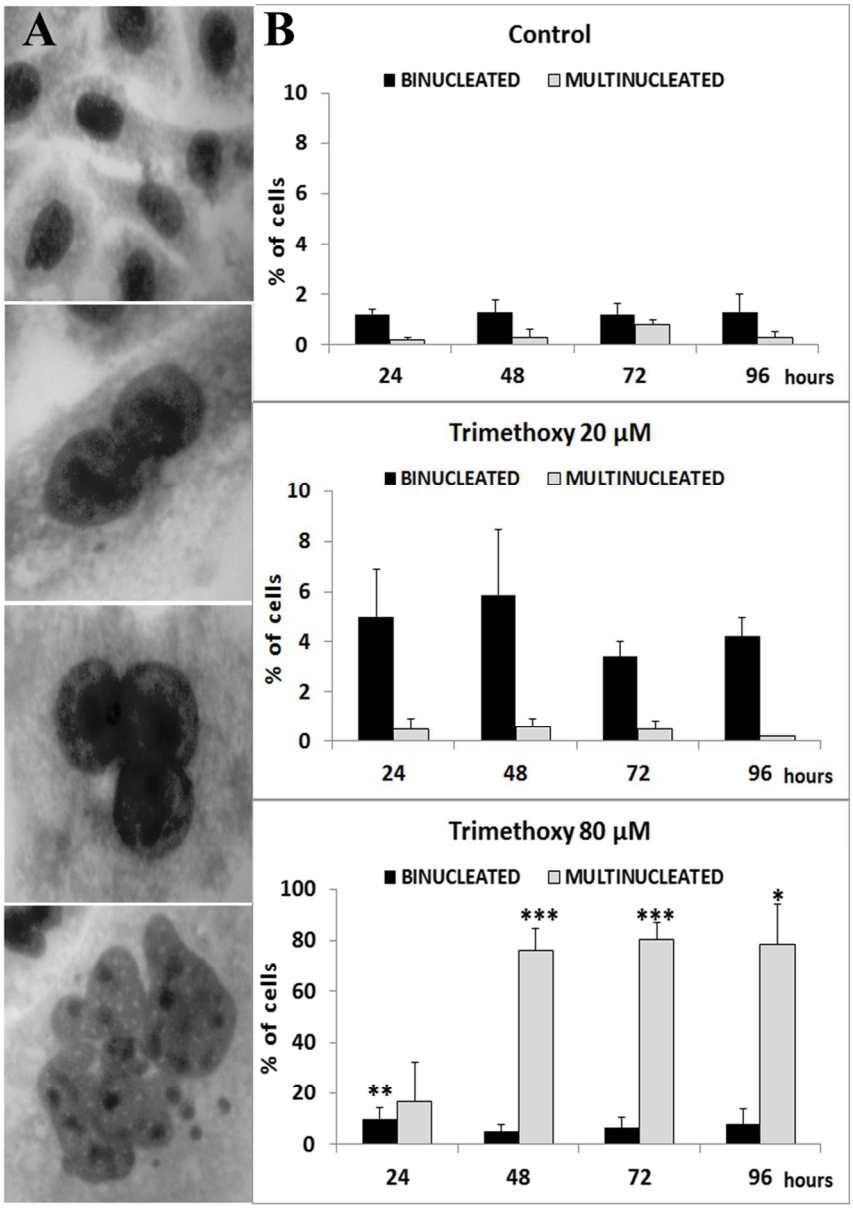

Figure 6. Induction of multinucleation by Trimethoxy in HeLa cells. Hela cells were treated for 24,48, 72 and 96 hours with Trimethoxy (20 and 80 µM). At the end of treatments cells were fixed and stained with Giemsa. (A) Microscopic images showing cells with 1, 2, 3 or more nuclei. (B) In the histograms the percentage of binucleated or multinucleated cells is shown. Values are the mean ± S.E. from three independent experiments. *p<0.05 **p<0.01 *** p<0.001 as compared to the control using unpaired t-test

85x120mm (300 x 300 DPI)